

- [7] J. J. Craig, "Adaptive control of manipulators through repeated trials," in *Proc. ACC*, San Diego, CA, June 1984, pp. 1566–1572.
- [8] P. Bondi, G. Casalino, and L. Gambardella, "On the iterative learning control theory for robotic manipulators," *IEEE J. Robot. Automat.*, vol. 4, pp. 14–22, Feb. 1988.
- [9] K. Guglielmo and N. Sadeh, "Theory and implementation of a repetitive robot controller with Cartesian trajectory description," *J. Dynam. Syst., Meas., Contr.*, vol. 118, pp. 15–21, Mar. 1996.
- [10] R. Horowitz, W. Messner, and J. B. Moore, "Exponential convergence of a learning controller for robot manipulators," *IEEE Trans. Automat. Contr.*, vol. 36, pp. 890–894, July 1991.
- [11] F. Lange and G. Hirzinger, "Learning accurate path control of industrial robots with joint elasticity," in *Proc. IEEE Conf. Robotics and Automation*, Detroit, MI, May 1999, pp. 2084–2089.
- [12] R. Horowitz, "Learning control of robot manipulators," *J. Dynam. Syst., Meas., Contr.*, vol. 115, pp. 402–411, June 1993.
- [13] K. L. Moore, *Iterative Learning Control for Deterministic Systems, Advances in Industrial Control*. New York: Springer-Verlag, 1993.
- [14] ———, "Iterative learning control—an expository overview," *Appl. Comput. Contr., Signal Processing, Circuits*, vol. 1, pp. 151–214, 1998.
- [15] Y. Chen and C. Wen, *Iterative Learning Control: Convergence, Robustness and Applications*. New York: Springer-Verlag, 1999, vol. 248.
- [16] Z. Bien and J.-X. Xu, *Iterative Learning Control: Analysis, Design, Integration and Application*. Norwell, MA: Kluwer, 1998.
- [17] N. Amann and D. H. Owens, "Non-minimum phase plants in iterative learning control," in *Proc. 2nd Int. Conf. Intelligent Systems Engineering*, Hamburg, Germany, 1994, pp. 107–112.
- [18] N. Amann, D. H. Owens, and E. Rogers, "Iterative learning control using prediction with arbitrary horizon," in *Proc. Eur. Control Conf., CD-ROM*, Brussels, Belgium, July 1997.
- [19] K. S. Lee and J. H. Lee, *Design of Quadratic Criterion-Based Iterative Learning Control*. In *Iterative Learning Control: Analysis, Design, Integration and Applications*, Z. Bien and J. Xu, Eds. Norwell, MA: Kluwer, 1998.
- [20] S. Gunnarsson and M. Norrlöf, "On the design of ILC algorithms using optimization," *Automatica*, vol. 37, pp. 2011–2016, 2001.
- [21] M. Norrlöf, "An adaptive iterative learning control algorithm with experiments on an industrial robot," *IEEE Trans. Robot. Automat.*, vol. 18, pp. 245–251, Apr. 2002.
- [22] J. H. Lee, K. S. Lee, and W. C. Kim, "Model-based iterative learning control with a quadratic criterion for time-varying linear systems," *Automatica*, vol. 36, no. 5, pp. 641–657, May 2000.
- [23] M. Togai and O. Yamano, "Analysis and design of an optimal learning control scheme for industrial robots: A discrete system approach," in *Proc. 24th IEEE Conf. Decision and Control*, Ft. Lauderdale, FL, Dec. 1985, pp. 1399–1404.
- [24] J. S. Park and T. Hesketh, "Model reference learning control for robot manipulators," in *Proc. IFAC 12th Triennial World Congr.*, Sydney, Australia, July 1993, pp. 341–344.
- [25] Y.-J. Liang and D. P. Looze, "Performance and robustness issues in iterative learning control," in *Proc. 32nd Conf. Decision and Control*, San Antonio, TX, Dec. 1993, pp. 1990–1995.
- [26] D. de Roover, "Synthesis of a robust iterative learning controller using an  $H_\infty$  approach," in *Proc. 35th Conf. Decision and Control*, Kobe, Japan, Dec. 1996, pp. 3044–3049.
- [27] S. Gunnarsson and M. Norrlöf, "On the use of learning control for improved performance in robot control systems," in *Proc. Eur. Control Conf., CD-ROM*, Brussels, Belgium, July 1997.
- [28] S. G. Norrlöf, "Some experiences of the use of iterative learning control for performance improvement in robot control systems," in *Preprints 5th IFAC Symp. Robot Control*, vol. 2, Nantes, France, Sept. 1997, pp. 379–383.
- [29] D. M. Gorinevsky, D. Torfs, and A. A. Goldenberg, "Learning approximation of feedforward dependence on the task parameters: Experiments in direct-drive manipulator tracking," in *Proc. ACC*, Seattle, WA, June 1995, pp. 883–887.
- [30] J. A. Frueh and M. Q. Phan, "Linear quadratic optimal learning control (LQL)," in *Proc. 37th IEEE Conf. Decision and Control*, Tampa, FL, Dec. 1998, pp. 678–683.
- [31] J. R. J. E. Dennis and R. B. Schnabel, *Numerical Methods for Unconstrained Optimization and Nonlinear Equations*. Englewood Cliffs, NJ: Prentice-Hall, 1983.
- [32] L. Ljung, *System Identification: Theory for the User*, 2nd ed. Englewood Cliffs, NJ: Prentice-Hall, 1999.
- [33] ———, *System Identification Toolbox—For Use With Matlab*. Natick, MA: The Math Works Inc., 1995.

## Design of Bilateral Teleoperation Controllers for Haptic Exploration and Telemanipulation of Soft Environments

Murat Cenk Çavuşoğlu, Alana Sherman, and Frank Tendick

**Abstract**—In this letter, teleoperation controller design for haptic exploration and telemanipulation of soft environments is studied. First, a new measure for fidelity in teleoperation is introduced which quantifies the teleoperation system's ability to transmit changes in the compliance of the environment. This sensitivity function is appropriate for the application of telesurgery, where the ability to distinguish small changes in tissue compliance is essential for tasks such as detection of embedded vessels. The bilateral teleoperation controller design problem is then formulated in a task-based optimization framework as the optimization of this metric, with constraints on free-space tracking and robust stability of the system under environment and human operator uncertainties. The control design procedure is illustrated with a case study. The analysis is also used to evaluate the effectiveness of using a force sensor in a teleoperation system.

**Index Terms**—Bilateral control design, haptics, telemanipulation of soft objects, teleoperation.

### I. INTRODUCTION

Previous research on teleoperation has focused on manipulation of hard objects. However, the design constraints are different in an application that involves manipulation of deformable objects. The stability-performance tradeoff is the main determinant of the control design for teleoperation systems, as it is in many other cases, and both performance and stability are inherently dependent on the task for which the system is designed. This letter addresses the issues in the design of bilateral controllers for telemanipulation of soft objects. The motivation behind this study is robotic telesurgery, where a surgical operation is performed by robotic instruments controlled by surgeons through teleoperation [1].

Compared with traditional teleoperation applications, such as hazardous material handling or assembly in space applications, telesurgery requires a very high level of fidelity. The operator's ability to haptically explore the surgical environment is extremely important, as surgeons rely on haptic sensation to detect embedded structures within tissue that are not visually observable, such as blood vessels, nerves, and tumors. Therefore, the main objective of telesurgical system design is achieving

Manuscript received January 23, 2002. This paper was recommended for publication by Associate Editor P. Dupont and Editor I. Walker upon evaluation of the reviewers' comments. This work was supported in part by the National Science Foundation under Grants IRI-95-31837, CISE CDA-9726362, and IIS-0083472, ONR under MURI Grant N14-96-1-1200, ARO under MURI Grant DaaH04-96-1-0341, NASA under STTR Grant NAS1-20288, and US Air Force Research Laboratory under Grant F30602-01-2-0588. This paper was partially presented at the IEEE International Conference on Robotics and Automation, Seoul, Korea, 2001, the ASME International Mechanical Engineering Congress and Exposition, Orlando, FL, 2000, and the International Symposium on Robotics with Applications, Maui, HI, June 2000.

M. C. Çavuşoğlu was with the Department of Electrical Engineering and Computer Sciences, University of California, Berkeley, CA 94720 USA. He is now with the Department of Electrical Engineering and Computer Sciences, Case Western Reserve University, Cleveland, OH 44106 USA (e-mail: cavusoglu@cwru.edu).

A. Sherman is with the Department of Bioengineering of the University of California, Berkeley, CA 94720 USA (e-mail: alanas@socrates.berkeley.edu).

F. Tendick is with the Department of Surgery, University of California, San Francisco, CA 94143 USA and the Department of Bioengineering, University of California, Berkeley, CA 94720 USA (e-mail: tendick@robotics.eecs.berkeley.edu).

Digital Object Identifier 10.1109/TRA.2002.802199

better fidelity through control design and the mechanical design of the system.

In this letter, the teleoperator controller design problem is explicitly formulated within a task-based optimization framework, where the control design is explicitly an optimization of a performance measure relevant to the particular task. This has been suggested by some researchers in the field but has not received the emphasis it deserves. For example, there is no earlier work where optimization has been explicitly formulated or performed with an objective function other than force and position tracking.

Most studies in the literature, with the possible exception of Colgate's impedance-shaping controller design [2], use the generic "ideal" teleoperator response as the performance objective. Yokokohji defined an ideal response, in which the goal of the control design was to match the position and forces at the master and slave manipulators exactly or through a virtual impedance [3]. Lawrence defined transparency as the ratio between the transmitted and environment impedances [4]. His design goal was to keep this ratio close to one over a maximal bandwidth. The resulting ideal controller, Lawrence showed, was equivalent to Yokokohji's ideal teleoperation controller. However, whether this particular choice of fidelity is best for a given task or not is a relevant question. It is important to use a task-based performance objective rather than seeking a generic "ideal" teleoperator response.

Human perceptual capabilities need to be considered as part of the performance objective as well. Daniel and McAree [5] took into account considerations for improved stimulation of the tactile and kinesthetic receptors during teleoperator controller design by modifying the filter in the force feedback path. Colgate [2] introduced impedance-shaping bilateral control as a means of "constructively altering the impedance of a task," for improved perception by the user.

In most of the works in the literature, passivity of the system [2]–[4], [6]–[8] or unconditional stability [9] is used as the means for ensuring the stability of the teleoperator while it is coupled with arbitrary passive systems, environment, and operator. However, this condition is restrictive since the class of all possible passive systems is quite general. If a smaller set of environment and human operator impedances are considered in the analysis, it may be possible to increase the fidelity of the system further.

In this letter, the control design is explicitly formulated as a constrained optimization, which is in the same spirit as  $H_\infty$  and  $\mu$  control design methodology of modern control theory. There are some earlier works in the literature that use the robust control theory framework to design teleoperation controllers. Kazerooni established an  $H_\infty$ -based framework to design a controller that transmits only force information and no position or velocity data [10]. Yan and Salcudean used  $H_\infty$  optimization to design controllers for motion scaling [11] and Hu *et al.* formulated the teleoperator control design as a convex  $H_\infty$  optimization problem [8]. Leung *et al.* used  $\mu$  synthesis to design controllers for teleoperation under time delay [12]. However, these works are explicitly based on perfect force and position tracking notion of ideal teleoperator response and do not develop a methodology which can incorporate different design objectives.

This letter addresses these points by proposing a new fidelity measure for a compliance discrimination task and developing a design methodology using robust control theory for task-based optimization of the teleoperation controller, focusing on telemanipulation of deformable objects. The new measure for fidelity in teleoperation quantifies the teleoperation system's ability to transmit changes in the compliance of the environment, incorporating human perceptual capabilities. This sensitivity function is appropriate for the application of telesurgery, where the ability to distinguish small changes in tissue compliance is essential for tasks such as detecting embedded vessels. The bilateral teleoperation controller design problem is then the

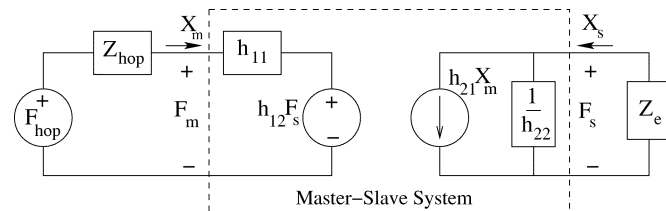


Fig. 1. Two-port input-output model and hybrid parameters of a teleoperation system.

optimization of this metric with constraints on free-space tracking and robust stability of the system under environment and human operator uncertainties. In this letter, we explicitly focus on telemanipulation in soft environments, limiting the set of possible human operator and environment impedances to improve fidelity as much as possible, since stability and performance trade off during control design. However, the control design and evaluation methodology that is presented is general, in the sense that it can be applied to different tasks or to manipulation of hard environments, by different choices of objective functions and stability conditions, for example, force and/or position tracking as the optimization objective and passivity of the teleoperator as the stability constraint.

## II. CONTROL DESIGN

### A. Formulation

The teleoperator can be modeled as a two-port network element relating force and position of the master manipulator,  $F_m$  and  $X_m$ , to the slave manipulator,  $F_s$  and  $X_s$ <sup>1</sup> (Fig. 1). We follow Hannaford [13] in using the hybrid parameters to characterize system behavior

$$\begin{bmatrix} F_m(s) \\ X_s(s) \end{bmatrix} = \begin{bmatrix} h_{11}(s) & h_{12}(s) \\ h_{21}(s) & h_{22}(s) \end{bmatrix} \begin{bmatrix} X_m(s) \\ F_s(s) \end{bmatrix}. \quad (1)$$

Environment impedance transmitted through the teleoperator can be calculated as

$$Z_t = \frac{F_m}{X_m} = \frac{h_{11} + (h_{11}h_{22} - h_{12}h_{21})Z_e}{1 + h_{22}Z_e} \quad (2)$$

using the hybrid parameters. Note that the impedances are defined as Force/Position not Force/Velocity. Here,  $Z_e$  is the environment impedance and  $F_s = -Z_e X_s$  as a result of the choice of the direction of  $X_s$ . We will consider a linear model as the underlying physical model throughout the analysis, which is only accurate locally.

### B. Task-Based Optimization Framework for Teleoperation Controller Design

The control design is formulated as the optimization problem of finding the controller values which optimize the fidelity of the teleoperation system with constraints on stability and tracking

$$\arg \sup_{\substack{\text{stability constraint} \\ \text{tracking constraint}}} \left( \begin{array}{c} \text{fidelity} \\ \text{measure} \end{array} \right). \quad (3)$$

*Fidelity* measure is the task-dependent measure of performance in teleoperation which is to be optimized during teleoperator controller design.

<sup>1</sup>In the literature, generally a force/velocity representation is used instead of a force/position representation. Although the force/velocity representation has the advantage that the power is immediately given by the terminal variables of the two port, it introduces a pole/zero pair at the origin causing complications in stability analysis conditions, which is purely an artifact of the representation. Here, the force/position representation is used to avoid these complications.

### C. Position Tracking as a Constraint

The tracking requirement is necessary to prevent the final controller parameter optimization from yielding trivial solutions,<sup>2</sup> as well as being a fundamental performance requirement in telemanipulation systems. Here, we will treat the position tracking requirement as a constraint in the form of having a specified minimum position tracking performance, rather than as part of a fidelity measure. This eliminates the need to combine the tracking error penalty with the task-based performance objective, using an arbitrary weight, to construct a fidelity measure.

We will pose this tracking requirement as a condition on the disturbance sensitivity function of the forward position loop during motion in free space. In the hybrid parameter formulation of the teleoperator, this sensitivity function is given by

$$S = 1 - h_{21}. \quad (4)$$

Then the tracking requirement can be posed as

$$|S(j\omega)| < |b(j\omega)| \iff \|SW_p\|_\infty \leq 1, \quad W_p = \frac{1}{b}(j\omega) \quad (5)$$

which dictates a tracking error less than  $|b(j\omega)|$  for a sinusoidal input with angular frequency  $\omega$  and magnitude one. This effectively puts a condition on the slave position gain when the slave is controlled by the master position (position only loop in the forward direction).

### D. Fidelity

In robotic telesurgery one would like to improve the ability to detect compliance changes in the environment in addition to the basic requirement of “good” tracking. This ability to detect compliance variations is critical in a surgical application. For example, the interaction of the needle with tissue during suturing, such as to feel when the needle punctures or leaves tissue, can be detected through a change in the perceived compliance. Also, structures hidden inside tissue, such as blood vessels, major nerves, or tumors, can be located by noninvasively probing the tissue. In these cases, it is more desirable to have the ability to detect changes in the environment impedance than simple position or force tracking between the master and slave manipulators. Therefore, it is necessary to introduce a fidelity measure that quantifies this ability.

The choice of fidelity metric is based on experiments in human perception of compliant surfaces by Dhruv and Tendick [14]. Although human subjects are poor at distinguishing the relative compliance of two surfaces (just-noticeable difference of 14%–25%), they can be very sensitive to changes as they haptically scan across a surface. In these experiments, compliance in the vertical direction was varied sinusoidally across a virtual simulated horizontal surface displayed with a haptic interface. As subjects scanned the surface, the spatial variation in compliance was converted to temporal oscillation. As temporal frequency increased, subjects’ sensitivity to compliance variation improved to better than 1% just-noticeable difference due to human vibration sensitivity.

Consequently, the measure of fidelity proposed in this letter is the sensitivity of the transmitted impedance to changes in the environmental impedance. This can be defined as

$$\left\| W_s \frac{dZ_t}{dZ_e} \Big|_{Z_e = \hat{Z}_e} \right\|_2 = \left\| W_s \frac{-h_{12}h_{21}}{(1 + h_{22}\hat{Z}_e)^2} \right\|_2 \quad (6)$$

<sup>2</sup>To illustrate the problem of trivial solutions, consider the case of optimizing a controller for transparency at a given environment stiffness as operating point. The trivial solution to this optimization is to have a master controller which gives the master manipulator an apparent stiffness equal to the nominal environment stiffness and have no feedback from slave to master, or even not actuate the slave at all.

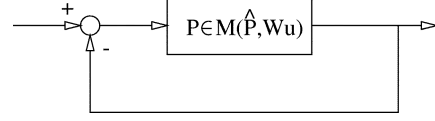


Fig. 2. Closed-loop system with multiplicative uncertainty.

where  $W_s$  is a frequency-dependent weighting function and  $\hat{Z}_e$  is the nominal environment impedance.

We use a low-pass filter with a cutoff frequency of 40 Hz as the weighting function  $W_s$ . This weighting function is based on the results of the experiments performed by Dhruv and Tendick [14] to measure the frequency dependence of the human operators’ force and compliance contrast-detection thresholds. In this study, the contrast-detection threshold was determined to decrease exponentially until 30 Hz–40 Hz, staying constant afterwards.<sup>3</sup>

### E. Stability

Any teleoperation system must maintain stability under operator and environment variations. In this letter, we focus on telemanipulation in soft environments, limiting the set of possible human operator and environment impedances, rather than considering all possible passive environment and human-operator impedance. This is done to be able to improve fidelity as much as possible, since stability and performance trade off during control design. In this section, we construct a simple norm condition to check robust stability of the system coupled with a specified set of environment and human-operator impedances. We use a robust stability criterion for unstructured uncertainties as given in Zhou, *et al.* [15]. For single-input/single-output (SISO) systems, the criterion is as follows.

*Theorem 1 (Robust Stability Criterion):* Consider the closed loop system shown in Fig. 2 with multiplicative unstructured uncertainty. The uncertainty is defined as

$$P \in M(\hat{P}, W_u) = \{\hat{P}(1 + W_u\Delta) : \Delta \in \mathcal{R}, \sup |\Delta(j\omega)| < 1, \# \text{ of rhp poles}(\hat{P}) = \# \text{ of rhp poles}(\hat{P}(1 + W_u\Delta))\} \quad (7)$$

where  $P$  is the loop gain,  $\hat{P}$  is the nominal plant loop gain,  $W_u$  is the uncertainty weighting function, and  $\mathcal{R}$  is the set of proper real rational functions. Then, the closed-loop system shown is stable for all  $P \in M(\hat{P}, W_u)$ , if and only if it is stable for the nominal plant  $\hat{P}$  and

$$\|W_u T\|_\infty \leq 1 \quad (8)$$

where  $T = \hat{P}/(1 + \hat{P})$ . The uncertainty weighting function  $|W_u(j\omega)|$  can be interpreted as the percentage uncertainty in  $\hat{P}$  at the frequency  $\omega$ .

For the teleoperation system, the loop gain  $P$  is calculated in Hanaford [16] as

$$P = \frac{-h_{12}h_{21}Z_e}{(h_{11} + Z_{hop})(1 + h_{22}Z_e)} \quad (9)$$

where  $Z_e$  and  $Z_{hop}$  are respectively the environment and human-operator impedances.

In this letter, we will consider the uncertainties in the human operator and environment impedances. First, consider the variation in the environment. Since  $Z_e$  appears as  $Z_e/(1 + h_{22}Z_e)$  in the loop gain

<sup>3</sup>It is important to note that in the study of Dhruv and Tendick [14], it is not clear if the flattening of the threshold after 40 Hz is due to psychophysical reasons or the limitations of the haptic interface used. However, since we use the same hardware platform, i.e., the Phantom haptic interface, in our study, this distinction does not have a practical consequence. Nevertheless, it is important to be aware of this fact for applications using different platforms.

expression, we proceed to put an upper bound to the variation in this term for the possible set of environments  $Z_e \in \mathcal{Z}_e$ .

Start with some manipulation

$$P = \frac{-h_{12}h_{21}Z_e}{(h_{11} + Z_{hop})(h_{22}Z_e + 1)} \quad (10)$$

$$= \underbrace{\frac{-h_{12}h_{21}}{(h_{11} + Z_{hop})}}_{\hat{P}} \underbrace{\frac{\hat{Z}_e}{h_{22}\hat{Z}_e + 1}}_{1+W_{ue}\Delta} \frac{h_{22}\hat{Z}_e + 1}{\hat{Z}_e} \frac{Z_e}{h_{22}Z_e + 1}. \quad (11)$$

Since we want to have the nominal environment  $\hat{Z}_e$  for  $\Delta = 0$ , we pick

$$W_{ue}\Delta = \frac{1 + h_{22}\hat{Z}_e}{\hat{Z}_e} \frac{Z_e}{1 + h_{22}Z_e} - 1 = \frac{1}{h_{22}\hat{Z}_e} \frac{Z_e - \hat{Z}_e}{\frac{1}{h_{22}} + Z_e} \quad (12)$$

then we pick an upper bound to  $W_{ue}$  for the possible environment values

$$\left| \frac{Z_e - \hat{Z}_e}{\frac{1}{h_{22}} + Z_e} \right| < |\Phi(j\omega)| \rightarrow W_{ue} = \frac{1}{h_{22}\hat{Z}_e} \Phi. \quad (13)$$

$\Phi$  can be a function of the controller values and other known variables present in  $h_{22}$ .

Similarly, for the operator impedance variation, we proceed to put an upper bound to the term  $1/(h_{11} + Z_{hop})$  for the possible set of operator impedances,  $Z_{hop} \in \mathcal{Z}_{hop}$ . We pick

$$W_{uh}\Delta = \frac{h_{11} + \hat{Z}_{hop}}{h_{11} + Z_{hop}} - 1 = \frac{\hat{Z}_{hop} - Z_{hop}}{h_{11} + Z_{hop}} \quad (14)$$

to have  $\hat{Z}_{hop}$  for  $\Delta = 0$ . Then, we can pick an upper bound

$$\left| \frac{\hat{Z}_{hop} - Z_{hop}}{h_{11} + Z_{hop}} \right| < |W_{uh}(j\omega)| \quad (15)$$

which can be a function of the known variables present in  $h_{11}$ .

The two uncertainty terms can be combined to give a single multiplicative uncertainty weighting function as

$$W_u = W_{ue} + W_{uh} + W_{ue}W_{uh}. \quad (16)$$

### F. Control Design Algorithm

The complete control design algorithm is given by

$$\arg \sup_{\substack{\|W_u T\|_\infty \leq 1 \\ \text{stable for } P \\ \|W_p S\|_\infty \leq 1}} \inf_{\hat{Z}_e \in \mathcal{Z}_e} \left\| W_s \frac{dZ_t}{dZ_e} \Big|_{\hat{Z}_e} \right\|_2. \quad (17)$$

The controller gains are chosen to optimize the fidelity among the set of controller values which satisfy stability and tracking requirements. The fidelity term is slightly modified from (6) to be more general, optimizing the worst case fidelity for a given set of environment values,  $\hat{Z}_e$ .  $\hat{Z}_e$  is the range of environments in which sensitivity of the transmitted impedance to environment impedance variations is desired.

This optimization can be done by choosing a specific controller architecture and then determining the specific controller gains by (17). It is important to note that this is not a convex optimization since  $\|W_s(dZ_t/dZ_e)\|_2$  is not convex in the controller parameters. Therefore, proper numerical techniques should be used during the computation. However, even though the fidelity metric used was not convex in controller parameters, the resulting optimization is well behaved, as can be observed from the fidelity plots in Fig. 6, and

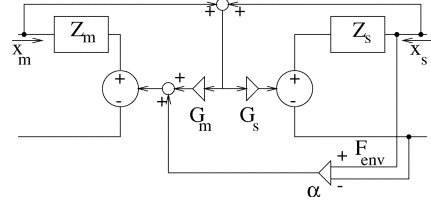


Fig. 3. P+FF architecture.

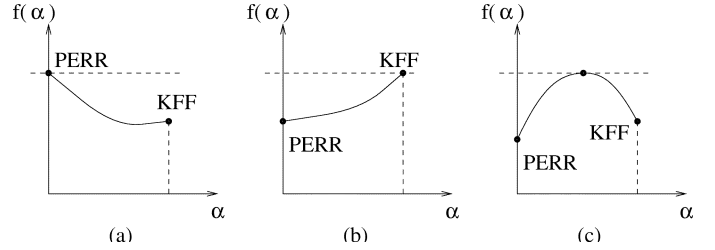


Fig. 4. Possible cases for the shape of  $\alpha$  curve.

does not cause significant computational problems. Using a specific controller limits the dimension of the parameter space and the stability constraint limits the size of the search space. A steepest-descent algorithm with multiple seed points successfully performs the optimization.

### III. COMPARING CONTROLLER ARCHITECTURES AND SENSORS

During the design of a telesurgical robot, we would like to know if the use of a force sensor on the slave manipulator is necessary for sufficient fidelity. For better performance, it is almost always desirable to use additional sensors; however, as this sensor will be located on the part of the instrument that will be inside the patient, it is a source of complications in the manipulator design and sterilization requirements, and adds to the cost of the final system.

Within this context, we will study the position error plus kinesthetic force feedback (P+FF) control architecture (Fig. 3). In the P+FF architecture, the master position is used to command the slave manipulator, and the force fed back to the master is a linear combination of the position error and the interaction force between the slave and the environment. The P+FF architecture is a hybrid of the position error-based force feedback (PERR) and kinesthetic-force feedback (KFF) architectures very frequently used in practical teleoperation applications. The PERR and KFF architectures are the limit cases of the more general control architecture P+FF. Therefore, it is possible to quantify the improvement due to using a force sensor for a given task by looking at how the fidelity of the P+FF architecture changes as the force gain is changed.

We define the  $\alpha$  curve as the highest fidelity achievable with the P+FF controller as a function of the force gain  $\alpha$ , subject to the stability and tracking constraints

$$f(\alpha) = \sup_{\substack{\|W_u T\|_\infty \leq 1 \\ \text{stable for } P \\ \|W_p S\|_\infty \leq 1 \\ G_m, G_s}} \inf_{\hat{Z}_e \in \mathcal{Z}_e} \left\| W_s \frac{dZ_t}{dZ_e} \Big|_{\hat{Z}_e} \right\|_2. \quad (18)$$

The shape of this curve depends on the stability constraint and the fidelity measure being used, as well as the hardware configuration itself. Therefore, it needs to be calculated for each case at hand. There are three cases based on location of the maximum point of the curve (Fig. 4). If the PERR end is the maximum, use of a force sensor does not improve performance. If the KFF end is the maximum, then it is

better to use purely the force sensor output as the source of force feedback. Finally, if the maximum is located at an intermediate point, it is possible to have better performance by using a combination of position error and the force measurements to generate force feedback. The relative value of the peak of the curve to the PERR value can be used to judge if the amount of performance improvement justifies the use of the force sensor.

#### IV. CASE STUDY

The testbed used to evaluate the analysis described above is a teleoperation system with two identical three-degree-of-freedom (DOF) robotic manipulators, Phantom v1.5 haptic interfaces (Sensible Technologies, Cambridge, MA) with custom motor drive electronics. The analysis here is carried out with a 1-DOF model, along the vertical direction, which is the axis orthogonal to the surface of the deformable body being manipulated. The local linear model of the manipulator in the vertical direction around the operating region is estimated as<sup>4</sup>

$$Z_m = Z_s = \frac{F}{X} = \frac{s^2 + 3.735s + 3.878 \times 10^{-4}}{1.168s^2 + 50.77s + 5.032 \times 10^4}. \quad (19)$$

This model is constructed from experimental black-box system identification.

The following environment and operator impedance variations are considered:

$$Z_e \in \{(B_e s + 1)K_e : 0 \leq B_e < \infty, 0 \leq K_e < \infty\} \quad (20)$$

$$Z_{hop} \in \left\{ \begin{array}{l} (M_{hop}s^2 + B_{hop}s + 1)K_{hop} : \\ 0 \leq M_{hop} \leq 0.05 \times 10^{-3}, \\ 0.021 \leq B_{hop} < \infty, 0.2 \leq K_{hop} \leq 2 \end{array} \right\} \quad (21)$$

with nominal impedances

$$\hat{Z}_e = 0.35(0.05s + 1) \quad (22)$$

$$\hat{Z}_{hop} = 1.51(0.05 \times 10^{-3}s^2 + 0.0219s + 1). \quad (23)$$

The range of  $Z_e$  represents environments from zero to infinite stiffness and damping. The nominal value of  $Z_e$  is the stiffness of the silicone gel we used in experimental evaluation of the teleoperation systems in [17], which is also within typically reported soft tissue stiffness values. The range and nominal value of  $Z_{hop}$  were partly experimentally determined from subjects using the haptic interface and partly estimated using the values reported in the literature [10], [18], [19].

The following upper bounds for the uncertainty terms of (13) and (15) are used in the stability analysis:

$$\Phi(s) = 10^{3/20} \frac{\frac{s^2 + 2 \times 0.1 \times 220 + 220^2}{220^2} \frac{s}{15} + 1}{\frac{s^2 + 2 \times 0.27 \times 105 + 105^2}{105^2} \frac{s}{1000} + 1} \quad (24)$$

$$W_{uh}(s) = 10^{16.7/20} \frac{\frac{s^2 + 2 \times 0.1 \times 208 + 208^2}{208^2} \frac{s}{200} + 1}{\frac{s^2 + 2 \times 0.5 \times 179 + 179^2}{179^2} 1}. \quad (25)$$

These upper bounds are determined by systematically varying the parameters  $G_s$ ,  $B_e$ , and  $K_e$  for (24), and  $G_m$ ,  $M_{hop}$ ,  $B_{hop}$ , and  $K_{hop}$  for (25) within their specified limits (see Fig. 5). The upper bound used for the tracking sensitivity function is

$$b(s) = \frac{Z_s}{0.25 + Z_s} \left( \frac{\frac{s}{95} + 1}{\frac{s}{160} + 1} \right)^3 \left( \frac{\frac{s}{160} + 1}{\frac{s}{250} + 1} \right)^3. \quad (26)$$

<sup>4</sup>All the units are in Newtons for force and millimeters for distance.

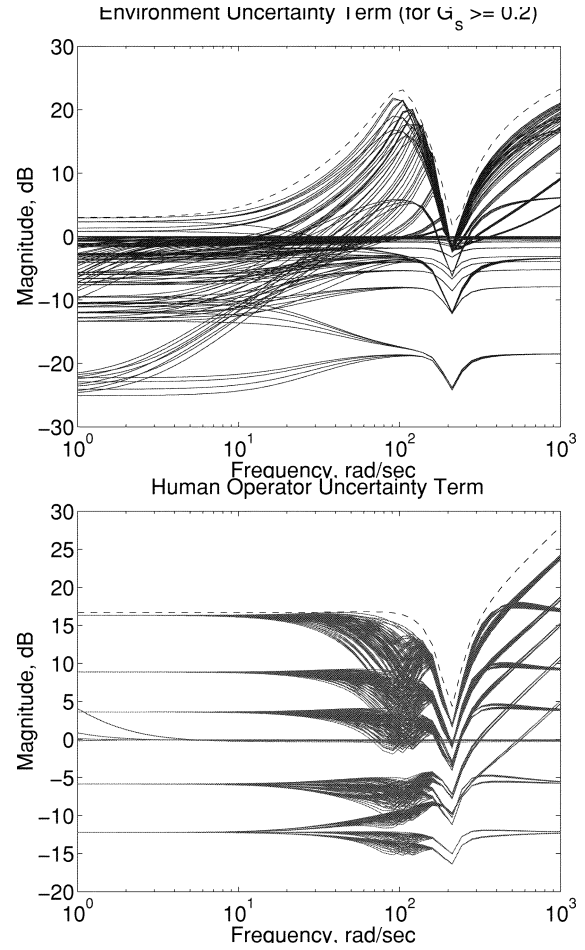


Fig. 5. Uncertainty weighting functions. (a) Environment uncertainty term. (b) Human operator uncertainty term. Dashed line is the upper bound for the uncertainty.

This upper bound requires good position tracking at low frequencies where the voluntary hand movements occur. The first term is chosen using the sensitivity function  $S$  at  $G_s = 0.25$  and the remaining terms are chosen to accommodate underdamped behavior occurring for  $G_s > 0.25$ . The resulting  $b(s)$  practically puts a lower bound on the slave position gain as  $G_s \geq 0.25$ .

It is important to note that the stability analysis performed with these upper bounds is conservative in the sense that it does not completely capture the dependence of the uncertainty weighting function on the known variables, such as controller gains. For example, the bound in (24) is chosen to be a constant transfer function, whereas it is actually possible to pick an upper bound which is a function of the controller gains. This dependence is a nontrivial function of controller gains, so a constant upper bound is used here.

It is also possible to find a single upper bound for the combined environment and operator uncertainties. However, the combined bound would have been completely independent of controller gains, whereas the bound constructed from pieces has some (even though not complete) dependence from (13), since  $h_{22}$  is a function of controllers. This gives a less conservative upper bound than we would get with a single constant term.

The fidelity plots for the KFF and PERR controllers superimposed with isostability curves are shown in Fig. 6. The fidelity-stability tradeoff can easily be observed on these plots, as the stability degrades as fidelity improves. The resulting  $\alpha$  curve is shown in Fig. 7. This curve predicts that using a force sensor will improve the performance

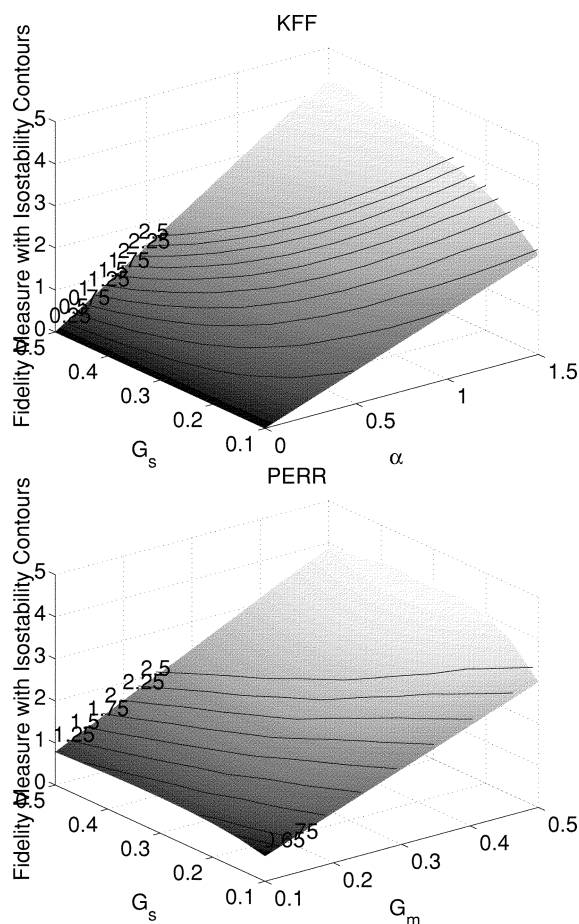


Fig. 6. Fidelity of the PERR and KFF architectures as a function of controller parameters. Contours of constant stability are shown overlaid on the fidelity surface for comparison. Note that stability decreases as fidelity increases.

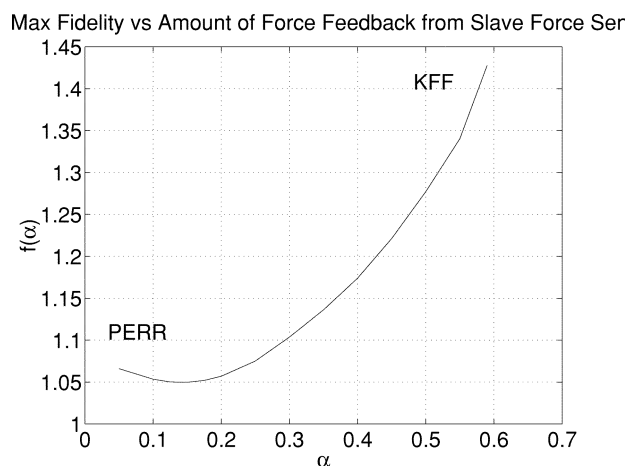


Fig. 7.  $\alpha$  curve for the teleoperation system studied.

and the KFF algorithm will perform best for the choice of the fidelity measure, tracking requirements and the uncertainty bounds considered.

## V. CONCLUSION

In the case study we have described, we have assumed a limited set of human-operator and environment uncertainties rather than, for example, requiring stability in contact with an arbitrary passive environ-

ment. This permits us to achieve better fidelity. It is possible, however, to encounter conditions beyond this limited set. For example, in robotic telesurgery, the slave manipulator could temporarily contact a rigid obstacle. However, under such conditions, the importance of fidelity becomes secondary to maintaining stability. The controller designed in the case study could be used as a local high-performance controller in a hierarchical design framework. Using a safety controller as suggested by Çavuşoğlu *et al.* [20] or a switching controller similar to that suggested by Hannaford and Ryu [21], the controller could switch to a high-stability, lower fidelity mode under such temporary conditions. If it is preferred to have a single controller instead of a hierarchical controller, one could choose the set of all passive environments for the stability criterion in Section II, but of course this would decrease performance.

It is important to note that the stability measure developed here is on the conservative side for the specified uncertainties, mainly due to modeling errors in the weighting functions. It was possible to manually increase the gains of the physical setup and still maintain stability. It may be more appropriate to use a structured uncertainty model to best capture this kind of uncertainty. Linear fractional transformations may provide a better framework to model the uncertainties.

We are also working on a more detailed model of the system which includes the noise and the dynamic characteristics of the force sensor which were not modeled in the analysis here. Including the nonidealities of the sensors is important to make a better comparison between the sensory schemes. For example, absence of noise in the force sensor model gives an unfair advantage to the KFF algorithm in the  $\alpha$  curve analysis. These modeling efforts will emphasize developing other quantitative means to compare sensory schemes.

Operator performance is one of the important components of teleoperator design. Therefore, experimental evaluation of control algorithms is crucial. The most prominent experimental studies are the experimental studies at the NASA Jet Propulsion Laboratory [22]–[24] and by Lawn and Hannaford [25] comparing various teleoperation algorithms within the context of operator performance. However, the experimental tasks used in these experiments are not suitable for evaluation of telesurgical systems. An experimental methodology to evaluate operator performance using teleoperation systems in a task more representative of surgery, complementing the control design procedure presented here, was presented by the authors in [17]. The task used was an inclusion-detection task to simulate the palpation of soft tissue during surgery, evaluating teleoperation systems in a compliance-discrimination task. This study was performed before the control design procedure had fully matured to the form presented here. To replicate these experiments with controllers designed using the full control design procedure presented here is one of the intended thrusts of our future research.

## REFERENCES

- [1] M. C. Çavuşoğlu, F. Tendick, M. Cohn, and S. S. Sastry, "A laparoscopic telesurgical workstation," *IEEE Trans. Robot. Automat.*, vol. 15, pp. 728–739, Aug. 1999.
- [2] J. E. Colgate, "Robust impedance shaping telemanipulation," *IEEE Trans. Robot. Automat.*, vol. 9, pp. 374–384, Aug. 1993.
- [3] Y. Yokokohji and T. Yoshikawa, "Bilateral control of master-slave manipulators for ideal kinesthetic coupling—Formulation and experiment," *IEEE Trans. Robot. Automat.*, vol. 10, pp. 605–620, Oct. 1994.
- [4] D. A. Lawrence, "Stability and transparency in bilateral teleoperation," *IEEE Trans. Robot. Automat.*, vol. 9, pp. 624–637, Oct. 1993.
- [5] R. W. Daniel and P. R. McAree, "Fundamental limits of performance for force reflecting teleoperation," *Int. J. Robot. Res.*, vol. 17, no. 8, pp. 811–830, Aug. 1998.
- [6] R. J. Anderson and M. W. Spong, "Bilateral control of teleoperators with time delay," *IEEE Trans. Automat. Contr.*, vol. 34, pp. 494–501, May 1989.
- [7] G. Niemeyer and J. J. E. Slotine, "Stable adaptive teleoperation," *IEEE J. Oceanic Eng.*, vol. 16, no. 1, pp. 152–162, Jan. 1991.

- [8] Z. Hu, S. E. Salcudean, and P. D. Loewen, "Robust controller design for teleoperation systems," in *Proc. IEEE Int. Conf. Systems, Man, Cybernetics*, vol. 3, Vancouver, BC, Canada, Oct. 1995, pp. 2127–2132.
- [9] R. J. Adams and B. Hannaford, "Stable haptic interaction with virtual environments," *IEEE Trans. Robot. Automat.*, vol. 15, pp. 465–474, June 1999.
- [10] H. Kazerooni, T.-I. Tsay, and K. Hollerbach, "A controller design framework for telerobotic systems," *IEEE Trans. Contr. Syst. Technol.*, vol. 1, pp. 50–62, Mar. 1993.
- [11] J. Yan and S. E. Salcudean, "Teleoperation controller design using H-infinity optimization with application to motion-scaling," *IEEE Trans. Contr. Syst. Technol.*, vol. 4, pp. 244–258, May 1996.
- [12] G. M. H. Leung, B. A. Francis, and J. Apkarian, "Bilateral controller for teleoperators with time delay via mu-synthesis," *IEEE Trans. Robot. Automat.*, vol. 11, pp. 105–116, Feb. 1995.
- [13] B. Hannaford, "A design framework for teleoperators with kinesthetic feedback," *IEEE Trans. Robot. Automat.*, vol. 5, pp. 426–434, Aug. 1989.
- [14] N. Dhruv and F. Tendick, "Frequency dependence of compliance contrast detection," in *Proc. Symp. Haptic Interfaces for Virtual Environment and Teleoperator Syst., ASME Int. Mech. Eng. Congr. Expo. (IMECE 2000)*, vol. DSC 69-2, Orlando, FL, Nov. 2000, pp. 1087–1093.
- [15] K. Zhou, J. C. Doyle, and K. Glover, *Robust and Optimal Control*. Englewood Cliffs, NJ: Prentice-Hall, 1996.
- [16] B. Hannaford, "Stability and performance tradeoffs in bi-lateral telemanipulation," in *Proc. IEEE Int. Conf. Robotics Automation*, Scottsdale, AZ, 1989, pp. 1764–1767.
- [17] A. Sherman, M. C. Çavuşoğlu, and F. Tendick, "Comparison of teleoperator control architectures for palpation task," in *Proc. ASME Dynamic Syst. Control Div., ASME Int. Mech. Eng. Congr. Expo. (IMECE 2000)*, vol. 2, Orlando, FL, Nov. 2000, pp. 1261–1268.
- [18] P. Buttolo, "Characterization of Human Pen Grasp With Haptic Displays," Ph.D. dissertation, Dept. Elect. Eng., Univ. Washington, 1996.
- [19] A. Z. Hajian and R. D. Howe, "Identification of the mechanical impedance at the human finger tip," *J. Biomech. Eng.*, vol. 119, pp. 109–114, Feb. 1997.
- [20] M. C. Çavuşoğlu, J. Yan, and S. S. Sastry, "A hybrid system approach to contact stability and force control in robotic manipulators," in *Proc. 12th IEEE Int. Symp. Intelligent Control (ISIC'97)*, Istanbul, Turkey, July 1997, pp. 143–148.
- [21] B. Hannaford and J.-H. Ryu, "Time domain passivity control of haptic interfaces," in *Proc. IEEE Int. Conf. Robotics Automation*, vol. 2, 2001, pp. 1863–1869.
- [22] H. Das, H. Zak, W. S. Kim, A. K. Bejczy, and P. S. Schenker, "Operator performance with alternative manual control modes in teleoperation," *Presence*, vol. 1, no. 2, pp. 201–218, Spring 1992.
- [23] W. S. Kim, B. Hannaford, and A. K. Bejczy, "Force-reflection and shared compliant control in operating telemanipulators with time delay," *IEEE Trans. Robot. Automat.*, vol. 8, pp. 176–185, Apr. 1992.
- [24] B. Hannaford, L. Wood, D. A. McAfee, and H. Zak, "Performance evaluation of a six-axis generalized force-reflecting teleoperator," *IEEE Trans. Syst., Man, Cybern.*, vol. 21, pp. 620–633, May/June 1991.
- [25] C. A. Lawn and B. Hannaford, "Performance testing of passive communication and control in teleoperation with time delay," in *Proc. IEEE Int. Conf. Robotics Automation*, Atlanta, GA, 1993, pp. 776–783.

## An Efficient Approach to the Forward Kinematics of a Planar Parallel Manipulator With Similar Platforms

Ping Ji and Hongtao Wu

**Abstract**—The forward kinematics of a parallel manipulator is so difficult that the analytical solutions of only a few parallel manipulators have been found. The forward kinematics of a three-degree-of-freedom planar parallel manipulator, where the base and the mobile platforms are two similar triangles, is studied in this paper and its analytical solution is provided. The final solution is two independent univariate quadratic equations. As well, the forward kinematics solution is simplified to the parallel manipulator where the two triangles are equilateral and a numerical example is presented.

**Index Terms**—Analytical solution, forward kinematics, parallel manipulator.

### I. INTRODUCTION

A three-degree-of-freedom (DOF) planar parallel manipulator, in general, consists of two triangles in a plane, as shown in Fig. 1. The moving triangle  $\Delta A_1 A_2 A_3$  is the mobile platform while three fixed points,  $B_1$ ,  $B_2$ , and  $B_3$ , form another triangle  $\Delta B_1 B_2 B_3$ , that is, the base platform. An extensible limb  $L_k$  links the couple vertices  $A_k$  and  $B_k$  ( $k = 1, 2, 3$ ). The mobile platform can rotate and move in the plane if the limbs change their lengths with actuators, either prismatic [1]–[3] or revolute [2]. This manipulator was first proposed by Gosselin and Merlet [4] and discussed by some researchers, including [1]–[10]. This paper only discusses the manipulator with prismatic actuators, called the RPR chains (R: revolute, P: prismatic) [5], [6]. Obviously, the parallel manipulator has three DOF. The forward kinematics to this manipulator is to find the position and orientation of the mobile platform with respect to the fixed base platform with the known limb lengths.

This manipulator seems to have a very simple structure. However, its forward kinematics is quite complicated. The result of its forward kinematics is a univariate sixth polynomial [2], so it has to be solved numerically. Consequently, its forward kinematics has at most six solutions. The singularity problem of this parallel manipulator was discussed by Collins and McCarthy [7]. A special case of the manipulator, where two triangles are equilateral, has been studied more deeply due to its symmetry [8]–[10]. The purpose of this paper is to present an analytical solution to the forward kinematics of the planar parallel manipulator with two equilateral triangles. The two triangles of the manipulator to be studied in this paper are only required to be similar, not necessarily equilateral. Certainly, the result obtained here can be applied to the equilateral-triangular manipulator, since it is a special case of the similar triangular manipulators. This paper discusses the manipulator with two similar platforms in plane, as shown in Fig. 1, while the generalization of this manipulator, that is, the manipulator with two similar platforms in space, has been discussed by some researchers, including [11].

Manuscript received May 18, 2001; revised November 28, 2001. This paper was recommended for publication by Associate Editor C. Gosselin and Editor I. Walker upon evaluation of the reviewers' comments. This work was supported by The Hong Kong Polytechnic University under Project G-T056.

P. Ji is with the Department of Industrial and Systems Engineering, The Hong Kong Polytechnic University, Hung Hom, Kowloon, Hong Kong (e-mail: mfpji@polyu.edu.hk).

H. Wu is with the Department of Mechanical Engineering, Nanjing University of Aeronautics and Astronautics, Jiangsu 210016, P. R. China.

Digital Object Identifier 10.1109/TRA.2002.802208